

LASERS

PACS numbers: 42.65.Re; 42.60.By; 42.60.Jf; 42.60.Lh
DOI: 10.1070/QE2010v040n05ABEH014241

Amplification of subpicosecond UV pulses in the multistage GARPUN-MTW Ti : sapphire – KrF laser system

V.D. Zvorykin, A.O. Levchenko, N.N. Ustinovskii

Abstract. **Terawatt 248-nm UV pulses with an energy of 0.62 J, a width of no more than 1 ps, and a divergence of 20 μrad have been obtained in the first experiments on the GARPUN-MTW Ti : sapphire – KrF laser system at double-pass amplification of frequency-tripled pulses from the Ti : sapphire front end in wide-aperture electron-beam-pumped KrF amplifiers. The contrast of short pulses relative to the amplified spontaneous emission is found to be $\sim 10^6$ for energy densities and $\sim 10^{11}$ for intensities. The specificity of short-pulse amplification in an active medium with fast population inversion recovery and advantages of amplification of trains of short pulses or short and long pulses are discussed. The peak power of single subpicosecond pulses in this laser system can be increased to 30 TW, and the focused beam intensity can be as high as 10^{20} W cm^{-2}.**

Keywords: *multistage laser system, wide-aperture KrF amplifier, electron beam pumping, amplification of single pulses and pulse trains.*

1. Specific features of amplification of short laser pulses in KrF amplifiers

Laser systems for amplifying chirped pulses in solid media (including parametric amplifiers) [1] make it possible to obtain near-IR ($\lambda \sim 1$ μm) ultrashort (femto- and picosecond) laser pulses (USLPs) with a tera- and petawatt peak power, which are necessary to solve many fundamental and applied problems in nonlinear optics, physics of high energy densities, charged particle acceleration, and laser thermonuclear fusion (LTF). As compared with these systems, USLP excimer laser systems (see [2, 3] and references therein) have a number of significant differences: short wavelength and high photon energy with a fairly wide amplification band for 50-fs pulses (for example, $\lambda =$ 248.5 nm, $h\nu = 5$ eV, and $\Delta\lambda \sim 2.5$ nm for KrF lasers); lower (by three orders of magnitude) saturation energy density $Q_s = h\nu/\sigma \simeq 2$ mJ cm^{-2} ($\sigma = 2.5 \times 10^{-16}$ cm^2 is the induced-radiation cross section at the B → X transition of the KrF molecule); short lifetime of the excited state and, correspondingly, of the population inversion recovery in the active medium (the B-state radiative lifetime $\tau_r = 6.5$ ns, and, with allowance for quenching collisions, $\tau_c \sim 2$ ns) [4]; and a small nonlinear refractive index n_2 of the gain medium (the latter parameter is responsible for the laser beam filamentation).

The energy Q_{opt} extracted by as single USLP of duration $\tau \ll \tau_c$ from an aperture unit area in KrF amplifiers in the optimal regime ($Q_{opt} = Q_s \ln(g_0/\alpha_{ns}) = 5-6$ MJ cm^{-2} [5], where the ratio of the small-signal gain to the insaturable absorption coefficient $g_0/\alpha_{ns} = 10 - 20$ only slightly changes with pumping [4]) is much lower than the USLP energy obtained in solid-state systems. However, at large (~ 1 m^2) apertures of the existing electron-beam-pumped KrF amplifiers or those intended as LTF drivers [6–10], an output energy of 50–60 J can be obtained by direct amplification of unchirped pulses without expensive compressors for USLP compression; these values are comparable with the USLP energy obtained in modern solid-state systems. Fast population inversion recovery in the active medium makes it possible to effectively amplify USLP trains following with an interval $\Delta t \geqslant \tau_c$, and the use of angular multiplexing [11] provides a multiple (according to the ratio of the pump pulse width $\tau_p = 100 - 250$ ns to the pulse repetition rate $\Delta t \sim 2$ ns) increase in the total energy and power peak on the target. Multiplexing allows one to differently combine nano- and picosecond (or subpicosecond) pulses and thus obtain a complex temporal profile of pulses on the target [12, 13], which is necessary for separate compression and heating of LTF targets in the regimes of electron-induced fast ignition [14] or ignition by a strong shock wave (shock ignition) [15, 16]. In the fast-ignition scheme the UV radiation of a KrF laser can be focused into a spot of smaller area ($S \propto \lambda^2$) in comparison with the IR radiation of solid-state lasers. This provides a gain in intensity ($I \propto \lambda^{-2}$) with preservation of the scaling parameter $I(\lambda/\lambda_{ir})^2 \sim 10^{19}$ W cm^{-2} (here $\lambda_{ir} = 1.06$ μm), a value necessary for accelerating electrons to ~ 1 MeV [3, 8]. In addition, the penetration depth of UV radiation in plasma is larger, due to which the fast-electron generation region is located closer to the center of the compressed target, because the critical electron concentration N_e obeys the law $N_e \propto \lambda^{-2}$.

Along with LTF, there is another important application, where the above-mentioned properties of KrF lasers are advantageous in comparison with solid-state USLP systems. Specifically, this is the formation of extended conducting plasma channels in order to switch long electric (lightning)

V.D. Zvorykin, A.O. Levchenko, N.N. Ustinovskii P.N. Lebedev Physics Institute, Russian Academy of Sciences, Leninsky prosp. 53, 119991 Moscow, Russia; e-mail: zvorykin@sci.lebedev.ru, levchenk@sci.lebedev.ru, ustin@sci.lebedev.ru

Received 11 November 2009; revision received 27 February 2010
Kvantovaya Elektronika **40** (5) 381 – 385 (2010)
Translated by Yu.P. Sin'kov

discharges [17, 18] and directly transfer microwave radiation through plasma waveguide [19, 20]. The high UV photon energy ($h\nu = 5$ eV), comparable with the ionisation potential of molecules, makes it possible to efficiently photoionise gases in two- and three-photon processes. Since the probabilities of these processes increase with increasing intensity according to a power law (with exponents of 2 and 3, respectively) [18], to maintain the gas in the ionised state when a high-voltage breakdown develops, it is reasonable to use UV USLPs in the form of a train or in combination with long pulses.

Single 3–4-TW UV USLPs with the highest peak powers were obtained in KrF amplifiers with a 42-cm aperture (pulse energy 0.25 J, width 0.7 ps) [7, 8] and 60-cm aperture (10 J, 3 ps) [9]. However, the main characteristic of double-pass wide-aperture KrF amplifiers – the dependence of the USLP output energy density Q_{out} on the input energy density Q_{in} – has not been experimentally investigated. A specific feature of these amplifiers is the high-intensity amplified spontaneous emission (ASE), which significantly reduces the population inversion in the active medium and saturates the gain [2]. Its values $g(x)$, depending on the ASE intensity distribution in the amplifier, can be several times smaller than the small-signal gain g_0, which is set by pumping. Long ($\tau \gg \tau_c$) pulses of sufficiently high intensity, amplified in the quasi-stationary regime, have an advantage over ASE, because they almost completely extract the energy from active medium, which is continuously regenerated due to the pumping. At the same time, short pulses ($\tau \ll \tau_c$) extract the energy accumulated during τ_c; moreover, single pulses are amplified along the amplifier length in a medium with a quasi-stationary gain profile $g(x)$, determined by the ASE intensity. The situation changes when a short-pulse train is amplified. In this case, all pulses, except for the first one, are amplified in the ASE-unperturbed medium after the population inversion recovery. To implement this regime, the interval between the pulses must be shorter than the transition time τ_{ASE} of ASE intensity distribution, which is $\sim 2l/c$ in a double-pass amplifier. In this case, we assume that the reflection from the laser chamber walls is small and that the ASE reflection from the highly reflecting back mirror, (located at a distance l from the amplifier input) plays a key role. For the characteristic value $l = 1.5$ m, $\tau_{ASE} = 10$ ns.

2. Experimental

Here, we report the results of the first experiments on amplification of subpicosecond pulses on the GARPUN-MTW system, which is composed of two cascades of wide-aperture KrF amplifiers, an electric-discharge master KrF oscillator (Lambda Physik EMG MSC 150) and the Start-248 M Ti : sapphire front end (Avesta-Project Ltd.) [2]. The GARPUN final amplifier with an active volume of $12 \times 18 \times 100$ cm is pumped by two counterpropagating pulsed electron beams with a FWHM of 75 ns, an electron energy of 350 keV, and a current density of 50 A cm^{-2}. The GARPUN output energy in the free running regime (1.4-atm Ar–Kr–F_2 mixture, specific pump power $W_b = 0.7$–0.8 MW cm^{-3}) is 100 J. A Berdysh preamplifier with a volume of $8 \times 8 \times 110$ cm, pumped under similar conditions ($W_b = 0.6 - 0.7$ MW cm^{-3}, working mixture pressure 1.8 atm), generates an energy of 25 J. A KrF master oscillator (pulse width 20 ns, energy 150 mJ) fires laser-triggered switches on high-voltage pulse-forming lines (which feed vacuum diodes) and synchronises the pulses of the front end with the amplifier pump pulses with an error of ± 5 ns. The front end, equipped with a BBO frequency converter into the third harmonic, generates pulses with a width of 60–100 fs, energy up to 0.5 mJ, and a repetition frequency of 10 Hz, at a wavelength tuned to the gain band center of KrF amplifiers. A single USLP, cut from a train, is supplied to the inputs of amplifiers at the instant when the pump pulse intensity is close to maximum.

Figure 1 shows the schematic of the experiment and the corresponding equipment for measuring the USLP energy and width, as well as the spectral and angular distributions of amplified radiation intensity. In the case of double-pass amplification the initial beam (8 mm in diameter) was transformed using dielectric-coated convex and concave mirrors so as to provide the amplifier aperture filling and beam focusing in the diaphragm plane of the spatial filter, which is located between the amplifying cascades. All transmitting optical elements (windows of amplifiers and spatial filters) were made of calcium fluoride, because this material is characterised by the lowest nonlinear absorption for USLPs with $\lambda = 248$ nm [21, 22].

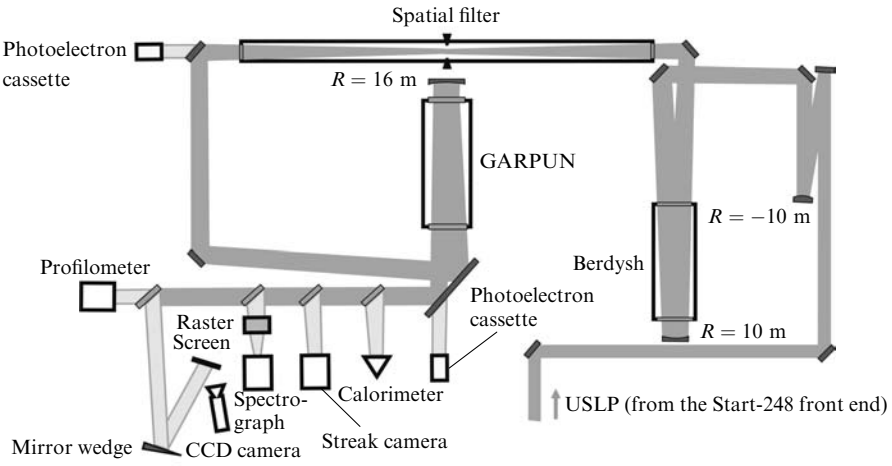

Figure 1. Schematic of the experiments on double-pass USLP amplification in KrF amplifiers.

3. Experimental results and discussion

Figure 2 shows the experimental dependences of the USLP energy density at the amplifier output (Q_{out}) on the corresponding values at the input (Q_{in}), in comparison with the calculated dependences for the given amplifier length L and different values of the small-signal gain g_0 and nonsaturable absorption α_{ns}. The incoherent USLP amplification was calculated using the modified Franz–Nodvik equation [5]:

$$\frac{df}{dx} = g(x)(1 - e^{f}) - \alpha_{ns}(x)f,$$

where

$$f = \frac{Q}{Q_s}; \quad Q(x) = \int_0^{\tau} I(x, t')dt';$$

for double-pass amplification ($0 < x < 2L$). The gain profiles $g(x)$ corresponded to those obtained in [2]. At the output of the GARPUN amplifier the ASE intensity I_{ASE} reached 5.2 MW cm^{-2}, which several times exceeded the saturation intensity $I_s = h\nu/(\sigma\tau_c) \approx 1.4$ MW cm^{-2} and reduced the gain by a factor of almost 5.

At the maximum value $Q_{out} = 0.6$ mJ cm^{-2} the Berdysh preamplifier operated in the nonsaturated regime and provided the total double-pass gain $G = Q_{out}/Q_{in} \approx 70$. The total output energy E_{out} reached 23 mJ; in this case the beam cross-section area (averaged over the preamplifier length), $S_1 = 38.5$ cm^2, was about 60 % of the preamplifier aperture S_a (i.e., the filling factor was $S_l/S_a = 0.6$). At high energy densities the saturation dependence $Q_{out}(Q_{in})$ deviates from the calculated one; this is apparently related to the nonlinear USLP absorption in the preamplifier windows. The final amplifier with $Q_{out} = 6.7$ mJ cm^{-2} worked in the saturation mode and produced a total energy of 0.62 J in a beam of area $S_l = 92.5$ cm^2 and aperture filling factor of 0.43.

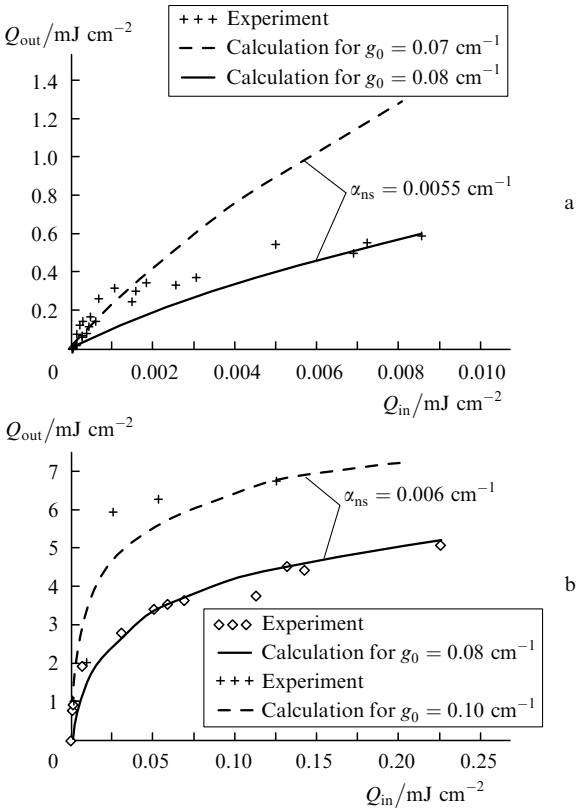

Figure 2. Dependences of the USLP output energy density Q_{out} on the input energy density Q_{in} for double-pass amplification (a) in the Berdysh preamplifier and (b) in the final GARPUN amplifier for two series of experiments.

The ASE energy, measured in the calorimeter solid angle ($\sim 2 \times 10^{-5}$ sr), was ~ 3 % of the USLP energy; this result is in agreement with the measurements and calculations of the ASE intensity angular distribution [2]. Optimisation of the amplification process (primarily, more complete filling of the amplifier aperture) is most likely to increase the single USLP energy to 1.5–2.0 J.

At a USLP width of 100 fs at the preamplifier input and the spectral width $\Delta\lambda = 0.75 - 0.80$ nm, the output pulse width was estimated to rise to 500 fs due to the group velocity dispersion in CaF_2 windows (their total thickness for double pass is 100 mm), as well as in air (path length 50 m). The output pulse width was determined in the experiments on the interference of the beams reflected from a thin mirror wedge (Fig. 3). A clear interference pattern became diffused at a gap of 100 μm, which corresponds to the 660-fs time of light double pass through the wedge. In fact this technique yielded the coherence length, which determines the estimation of the USLP width from below: $\tau_{1/2} \approx 330$ fs. After the double-pass USLP amplification in both amplifiers with a total thickness of CaF_2 windows of 200 mm the increase in the pulse width was evaluated to be 1 ps. The measurements with a UV streak camera (developed at the General Physics Institute, Russian Academy of Sciences), which has a limited time resolution, showed that the upper width limit in this case is $\tau_{1/2} \leqslant 1$ ps.

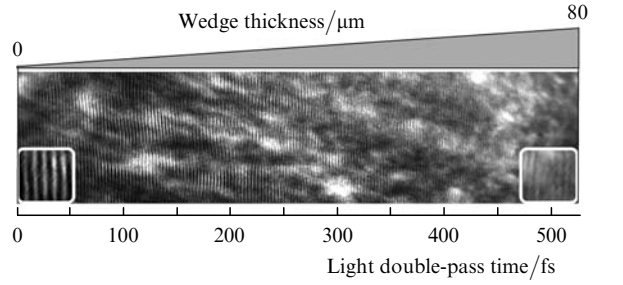

Figure 3. Interference pattern at USLP reflection from a mirror wedge.

The USLP intensity distributions in the near (Fig. 4) and far (Fig. 5) zones were recorded on a photographic paper located at different distances from the final amplifier in the convergent laser beam, formed after the reflection from the concave back mirror of the amplifier. To construct the distribution in the far zone, we processed series of focal spots obtained at a distance of 20 m from mirror after the multiple reflection of attenuated radiation in the mirror wedge. The distribution of the USLP intensity transmitted through the optical channel in the absence of pumping was measured in the same scheme using an OPHIR profilometer. A comparison of the measurement results showed that the pumping of amplifiers does not affect much the amplified beam divergence, which is mainly determined by the block structure of the CaF_2 laser windows and the corresponding

beam filamentation. The latter manifests itself in a slightly focused beam as a set of hot spots, concentrated along the image of block boundaries (Fig. 4). In reality, the peak radiation power in our case ($P \sim 1$ TW) greatly exceeds the critical power $P_{cr} = 3.8\lambda^2/(8\pi n_0 n_2) \approx 100$ MW for UV radiation with $\lambda = 248$ nm in air, where $n_0 \approx 1$ and $n_2 \approx 10^{-18}$ cm^2 W^{-1} are, respectively, the linear and nonlinear refractive indices of air [23].

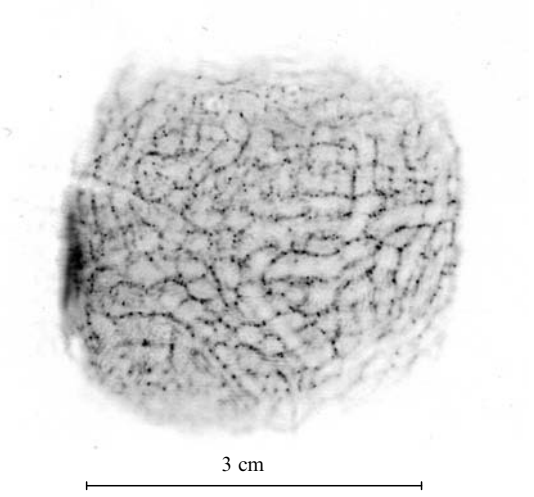

Figure 4. Amplified USLP intensity distribution in the near zone.

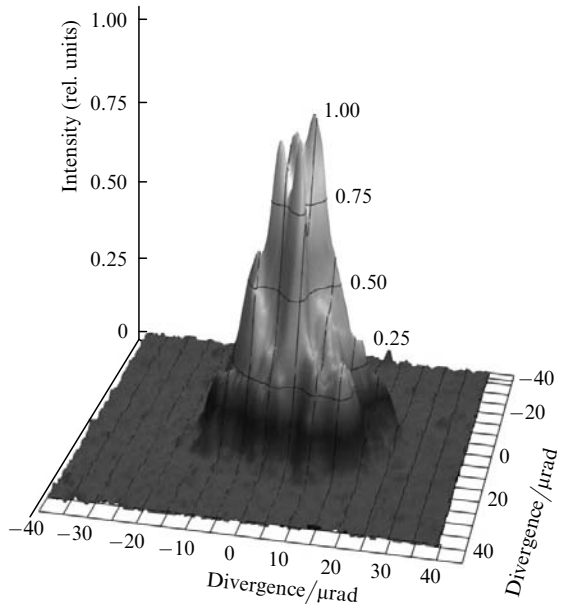

Figure 5. Amplified USLP intensity distribution in the far zone.

The USLP contrast with respect to ASE for a laser beam focused on the target was estimated (using the experimentally measured ASE intensities and beam divergence $\Theta_{1/2} = 20$ μrad and taking into account the solid angle ratio) to be $\sim 10^6$ for the energy densities and $\sim 10^{11}$ for the intensities. In the latter case we took into account the ASE FWHM (~ 40 ns).

The USLP spectral distribution was measured with a resolution of 0.01 nm on a DFS-457 spectrograph with a CCD array. A prism raster was installed at the entrance slit to randomise laser beam inhomogeneities. The ASE spectrum recorded in the absence of USLP at the input of the system had a maximum near $\lambda = 248.5$ nm and a half-width $\Delta\lambda_{1/2} \sim 0.25$ nm, a value much smaller than the linewidth of the B → X transition due to the high amplification in the channel. As a result of the nonlinear interaction with the amplifier windows and spatial filter, the spectral width of the USLPs transmitted through the optical channel without amplification increased to 1.2 nm in comparison with the initial value $\Delta\lambda_{1/2} \sim 0.75 - 0.80$ nm at the output of the front end. After the amplification the USLP spectrum became irregular, and its width increased to 2.3 nm, which approximately corresponds to the laser transition linewidth (Fig. 6). In principle, this gives grounds to expect pulse shortening to 50 fs if the dispersion spread in the windows can be compensated for by a negative frequency chirp, previously introduced into initial pulse with the aid of a prism stretcher [2]. Then the peak USLP power should increase to 30 TW after the amplification, which would make it possible to obtain beam intensities up to 10^{20} W cm^{-2} on the target, provided that the beam quality is improved (CaF_2 windows are replaced with single-block ones).

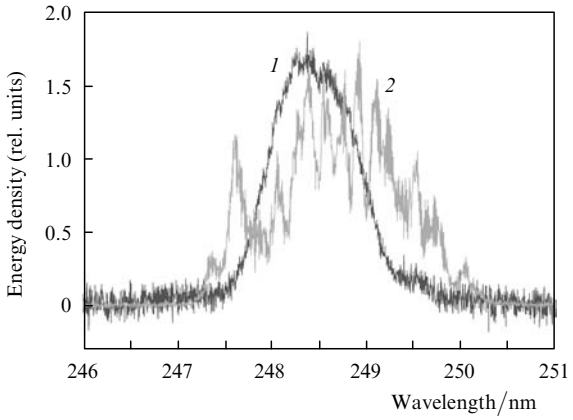

Figure 6. Spectral distribution of the USLP energy density (*1*) without amplification and (*2*) after amplification.

4. Conclusions

The amplification of single subpicosecond pulses in the GARPUN-MTW Ti : sapphire – KrF laser system in the double-pass scheme with two wide-aperture electron-beam-pumped KrF amplifiers was investigated. Terawatt 248-nm UV pulses with an energy of 0.62 J, width less than 1 ps, and a divergence of 20 μrad were obtained at the output of the system. The ASE-limited short-pulse contrast was found to be $\sim 10^6$ for energy densities and $\sim 10^{11}$ for intensities. Optimisation of the amplifiers will make it possible to increase the output energy to 1.5 – 2.0 J and to improve the laser beam quality. The measured spectral width of amplified pulse suggests that it can be shortened to 50 fs and the peak power can be increased to 30 TW by introducing a negative frequency chirp into the initial pulse. The focused beam intensity on the target may reach $\sim 10^{20}$ W cm^{-2} for such pulses. In summary, we should note again that a single USLP transfers only a small part (~ 0.02) of the energy accumulated in the active medium

during pumping of the KrF amplifiers (it is determined by the τ_c/τ_p ratio). The rest of the energy is generally released in the form of ASE into a wide solid angle; this emission deteriorates the short-pulse contrast. Instead, it can be used to amplify an USLP train or nanosecond pulses. In the case of USLP train amplification, the ASE effect is significantly reduced when the pulse repetition rate is equal to the time of population inversion recovery in the active medium ($\Delta t \approx \tau_c \approx 2$ ns) or at least shorter than the transition time of quasi-stationary ASE intensity (10 ns).

Acknowledgements. We are grateful to G.A. Mesyats, O.N. Krokhin, A.N. Starodub, and A.A. Ionin for the equipping of the GARPUN laser system with the Ti : sapphire front end and for the support of this study; to L.V. Seleznev and D.V. Sinitsyn for the preparation of the front end and the help in the experiments on subpicosecond pulse amplification; and to M.Ya. Shchelev and N.S. Vorob'ev for supplying the streak camera and the help in the measurements. This work was supported by the programs for basic research 'Problems of Physical Electronics of Charged-Particle Beams and Generation of Electromagnetic Radiation in High-Power Systems' and 'Extreme Light Fields and Their Applications' of the Presidium of the Russian Academy of Sciences and the Russian Foundation for Basic Research (Grant Nos 08-02-01331, 09-02-12018 ofi-m, and 09-07-13593-ofi-ts).

References

1. Strickland D., Mourou G. *Opt. Commun.*, **56**, 219 (1985).
2. Zvorykin V.D., Didenko N.V., Ionin A.A., et al. *Laser and Particle Beams*, **25**, 435 (2007).
3. Foldes I.B., Szatmari S. *Laser and Particle Beams*, **26**, 575 (2008).
4. Molchanov A.G. *Trudy FIAN*, **171**, 54 (1986) [*Proc. Lebedev Phys. Ins.*, **171**, 72 (1988)].
5. Tilleman M.M., Jacob J.H. *Appl. Phys. Lett.*, **50**, 121 (1987).
6. Rosocha L.A., Bowling P.S., Burrows M.D., et al. *Laser and Particle Beams*, **4**, 55 (1986).
7. Divall E.J., Edwards C.B., Hirst G.J., et al. *J. Mod. Opt.* **43**, 1025 (1996).
8. Shaw M.J., Ross I.N., Hooker C.J., et al. *Fusion Engineering and Design*, **44**, 209 (1999).
9. Owadano Y., Okuda I., Matsushima E., in *Inertial Fusion Sciences and Applications 2001* (Amsterdam: Elsevier, 2001) p. 465.
10. Obenschain S.P., Colombant D.G., Schmitt A.J., et al. *Phys. Plasmas*, **13**, 056320 (2006).
11. Lowenthal D.D., Ewing J.J., Center R.E., et al. *IEEE J. Quantum Electron.*, **QE-17**, 1861 (1981).
12. Zvorykin V.D., Lebo I.G., Rozanov V.B. *Kr. Soobshch. Fiz. FIAN*, (9 – 10), 20 (1997) [*Bull. Lebedev Phys. Inst.*, (9 – 10), 20 (1997)].
13. Lehmberg R.H., Giuliani J.L., Schmitt A.J. *J. Appl. Phys.*, **106**, 023103 (2009).
14. Basov N.G., Gus'kov S.Yu., Feoktistov L.P. *J. Russian Laser Research*, **13**, 396 (1992).
15. Shcherbakov V.A. *Fiz. Plazmy*, **9**, 409 (1983) [*Plasma Phys.*, **9**, 240 (1983)].
16. Obenschain S.P., Sethian J.D., Schmitt A.J. *Fusion Sci. Tech.*, **56**, 594 (2009).
17. Zhao X.M., Wang Y.C., Diels J.-C., Elizondo J. *IEEE J. Quantum Electron.*, **31**, 599 (1995).
18. Zvorykin V.D., Ionin A.A., Kudryashov S.I., et al. *Proc. 51st Workshop of the INFN ELOISOTRON* (Erice, Italy: World Scientific, 2008) p. 813.
19. Chateauneuf M., Payeur S., Dubois J., Kieffer J.-C. *Appl. Phys. Lett.*, **92**, 091104 (2008).
20. Zvorykin V.D., Levchenko A.O., Ustinovskii N.N., Smetanin I.V. *Pisma Zh. Eksp. Teor. Fiz.*, **91**, 244 (2010) [*JETP Lett.*, **91**, 226 (2010)].
21. Tomie T., Okuda I., Yano M. *Appl. Phys. Lett.*, **55**, 325 (1989).
22. Simon P., Gerhardt H. *Opt. Lett.*, **14**, 1207 (1989).
23. Khan N., Mariun N., Aris I., Yeak J. *New J. Phys.*, **4**, 61.1 (2002).